P-ISSN 2586-9000
E-ISSN 2586-9027
Homepage : *https://tci-thaijo.org/index.php/SciTechAsia* Science & Technology Asia
Vol.29 No.2 April-June 2024 Page: [63-73]
Original research article

Using Digital Image Correlation (DIC) in MATLAB Monitoring Number and Size of Speckle Granules

Siripon Kaoroptham[1,*], Rittipol Chantarat[2], Prapot Kunthong[3]

[1]*Department of Industrial Technology and Innovation Management, Faculty of Science and Technology, Pathum Wan Institute of Technology, Pathum Wan 10330, Thailand*
[2]*Department of Mechanical Engineering, Faculty of Engineering, Rajamangala University of Technology Rattanakosin, Nakhonprathom 73170, Thailand*
[3]*Department of Mechanical Engineering, Faculty of Engineering, Kasetsart University, Bangkok 10900, Thailand*

Received 15 January 2024; Received in revised form 25 February 2024
Accepted 1 April 2024; Available online 25 June 2024

ABSTRACT

This research aims to study the effect of changing the number and size of speckle granules to compare the result of the material properties between using the Digital Image Correction method (DIC) in MATLAB and the standard average of material properties. This research used stainless steel - grade 304 (UNS S30400) by testing 3 sets of experiments with an unequal number and size of speckle granules in each test to compare the effect of the number and size of speckle granules in calculations using Digital Image Correlation (DIC). The results show that the errors of changing the number of speckle granules from Digital Image Correlation (DIC) in Young's Modulus ($\boldsymbol{E}$) around 0.017238407-0.063998425% and Poisson's ratio ($\boldsymbol{\vartheta}$) around 0.072674419-1.251840943% and the errors of changing the size of speckle granules from Digital Image Correlation (DIC) in Young's Modulus ($\boldsymbol{E}$) around 0.030729470-0.316238141% and Poisson's ratio ($\boldsymbol{\vartheta}$) around 0.069043207-0.531703259%.

Keywords: Displacement DIC; Poisson's ratio DIC; Young's modulus DIC

1. Introduction

In the past, the material properties calculations were complex and related to many theories to find the answers. Both in mathematical numerical calculation systems and in applied physics systems, which makes it difficult to analyze and synthesize data to find answers or engineering solutions.

This research aims to study the material properties with the Digital Image Correlation (DIC) technique. The Digital Image Correlation (DIC) is an optical tech-

***Corresponding author:** siripon.k@ku.th

nique used for non-contact measurement of deformation, displacement, strain, and structure. DIC enables the analysis of how objects or materials deform and move under various conditions by tracking patterns in digital images. DIC is one of the tools in experimental mechanics, materials science, and structural engineering due to its ability to provide full-field measurements with high spatial resolution.

In addition, the effect of changing the number and size of speckle granules to compare the result of the material properties between using the digital image correction method (DIC) and the standard average of material properties.

Moreover, this research used stainless steel - grade 304 (UNS S30400) by testing 3 sets of experiments with an unequal number and size of speckle granules in each test to compare the effect of the number and size of speckle granules and the displacement in calculations using Digital Image Correlation (DIC).

2. Materials and Methods

Digital Image Correlation (DIC) relies on mathematical principles to calculate displacement and strain based on the analysis of pixel intensity patterns in digital images. The basic principles can be summarized with equations that describe the correlation process and subsequent calculation.

In this method, material is sprayed with speckles of paint to create a random speckle distribution, causing each piece of spray-painted speckle to have a different appearance, and then recorded with a digital camera.

The image shows that an image of the workpiece that has not been deformed and then begins to apply force to the material. The paint spot is sprayed will move along the removal distance on the surface of the material. Then the material will be photographed at the same location again.

Moreover, we define the scope of the study by framing the area of interest in photographs of undeformed and deformed material. We use the principle of comparing data by pixel points by storing data for workpieces that have not been deformed in the function $f(x,y)$ and pixel points of the workpiece that are deformed are in the function $g(x+.u, y+v)$ obtained from correlation (Cross-Correlation Coefficient) as shown in Fig.1.

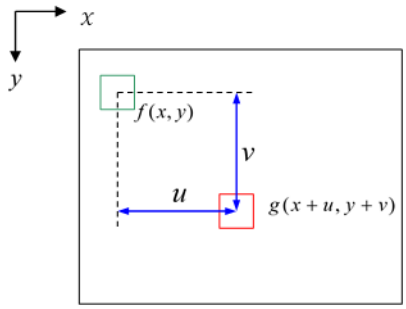

Fig.1. Cross-Correlation Coefficient [1].

By finding the correlation value We can find it from Eq. (2.1) by using calculations from the size frame $(2i+1)\times(2j+1)$ pixels.

$$C(u,v) = \frac{\sum_{x=-i}^{i}\sum_{y=-j}^{j}\left[\left(f(x,y)-f_m\right)\left(g(x+u,y+v)-g_m\right)\right]}{\sqrt{\left(\sum_{x=-i}^{i}\sum_{y=-j}^{j}\left(f(x,y)-f_m\right)^2\right)\times\left(\sum_{x=-i}^{i}\left(g(x+u,y+v)-g_m\right)^2\right)}}, \quad (2.1)$$

where $f(x,y)$ and the function $g(x+u,y+v)$ are the amount of light intensity (Gray Values), u and v are the displacements on the x and y axes of each pixel, and f_m and g_m are the average light intensity values.

To improve the accuracy of digital image correction (DIC) methods to less than 1 pixel, or sub-pixel accuracy we can use the correlation method along with the Newton-Rapson method. It was used by bicubic spline interpolation that was discovered by [2]. The light intensity of the image of the undeformed workpiece and the image of the deformed workpiece as shown in Eq. (2.2).

$$f(x,y) = \sum_{m=0}^{3}\sum_{n=0}^{3} a_{mn} x^m y^n, \qquad (2.2)$$
$$g(\tilde{x},\tilde{y}) = \sum_{m=0}^{3}\sum_{n=0}^{3} b_{mn} \tilde{x}^m \tilde{y}^n,$$

where (x,y) is the position of the pixel in each point of the undeformed workpiece image, $(\tilde{x},\tilde{y})$ is the position of the pixel in each point of the deformed workpiece, $x^m y^n$ are the four corners of unit square of the undeformed workpiece image, $\tilde{x}^m \tilde{y}^n$ are the four corners of unit square of the deformed workpiece image, and a_{mn} and b_{mn} are the junction constant can be determined by quantifying the light intensity across the gradient of each pixel.

This research is based on forces acting on workpieces in two dimensions. In general, measuring the deformation of a workpiece is an important aspect of predicting lifetime of subjects because, the workpiece is subjected to force, the workpiece will deform. One of the accepted methods is the Newton-Raphson method. The advantage of the N-R Method is that it allows for better accuracy in studying the removal of workpieces by using second and third order tailor series for calculation. The estimation is shown to find the elimination value as shown in Fig. 2. We consider point P to be a point that has not yet undergone deformation and is in the ordered pair $\left(x_p, y_p\right)$. Moreover, when deformation occurs, its position changes to $\tilde{P}$ and is in the form of ordered pair $\left(x_{\tilde{p}}, y_{\tilde{p}}\right)$ and the relationship of the movement of such ordered pairs can be represented by Eq. (2.3).

$$\begin{aligned} x_{\tilde{p}} &= x_p + U_p, \\ y_{\tilde{p}} &= y_p + V_p, \end{aligned} \qquad (2.3)$$

where U_p and V_p are the positions of the intersections of the point Pin the x and y directions.

For approximate the values of $U_{(x,y)}$ and $V_{(x,y)}$, we can use the ordered Taylor's series in Eq. (2.4).

$$\begin{aligned} U(x,y) &= U\left(x_p, y_p\right) + \left(x + x_p\right)\left.\frac{\partial U}{\partial x}\right|_{x_p, y_p} \\ &\quad + \left(y + y_p\right)\left.\frac{\partial U}{\partial y}\right|_{x_p, y_p}, \\ V(x,y) &= V\left(x_p, y_p\right) + \left(x + x_p\right)\left.\frac{\partial V}{\partial x}\right|_{x_p, y_p} \\ &\quad + \left(y + y_p\right)\left.\frac{\partial V}{\partial y}\right|_{x_p, y_p}. \end{aligned} \qquad (2.4)$$

From Fig. 2, if we consider the point Q in a pixel that has not yet undergone deformation, it is represented by the ordered pair $\left(x_Q, y_Q\right)$. When deformation occurs to the point $\tilde{Q}$ it is represented by the ordered pair $\left(x_{\tilde{Q}}, y_{\tilde{Q}}\right)$, where point $\tilde{Q}$ is related to point P as in Eq. (2.5).

$$\begin{aligned} x_{\tilde{Q}} &= x_p + \Delta x + U_Q, \\ y_{\tilde{Q}} &= y_p + \Delta y + V_Q, \end{aligned} \qquad (2.5)$$

where U_Q and V_Q are the positions of elimination at point Q in the x and y directions, $\Delta x = x_Q + x_p$ and $\Delta y = y_Q + y_p$ substitute Eq. (2.4) used to estimate U_p and V_p. Then substitute into Eq. (2.5) and it can be reformulated into Eq. (2.6).

$$\begin{aligned} x_{\tilde{Q}} &= \tilde{x} + U_p + \left.\frac{\partial U}{\partial x}\right|_{x_p, y_p} + \Delta x + \left.\frac{\partial U}{\partial y}\right|_{x_p, y_p} \Delta y, \\ y_{\tilde{Q}} &= \tilde{y} + V_p + \left.\frac{\partial V}{\partial x}\right|_{x_p, y_p} + \Delta x + \left.\frac{\partial V}{\partial y}\right|_{x_p, y_p} \Delta y. \end{aligned} \qquad (2.6)$$

For finding locations other than point Q, it can be written the equation in the form of Eq. (2.7).

$$\tilde{x} = x + u + \frac{\partial u}{\partial x}\Delta x + \frac{\partial u}{\partial y}\Delta y\ldots,$$
$$\tilde{y} = y + v + \frac{\partial v}{\partial x}\Delta x + \frac{\partial v}{\partial y}\Delta y\ldots, \qquad (2.7)$$

where $\tilde{x}$ and $\tilde{y}$ are the positions of any deformation in the considered frame, x and y are the positions before the deformation, $u, \frac{\partial u}{\partial x}, \frac{\partial u}{\partial y}, v, \frac{\partial v}{\partial x}, \frac{\partial v}{\partial y}$ is the gradient of the displacement at the center of the considered frame, and $\Delta x = \left(x - x_p\right)$ and $\Delta y = \left(y - y_p\right)$ are the distance in the moving frame at the coordinate (x, y).

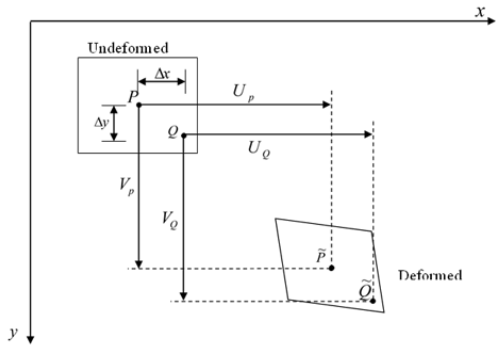

Fig. 2. The picture shows the frames of deformation and non-deformation [1].

Next step, the distribution of gray points represented by an ordered pair (x, y), the displacement is generated from the pre-deformation image represented by the function $f(x, y)$ and the deformation image generated can be represented by the function $g(\tilde{x}, \tilde{y})$. It can be written in the form of Eq. (2.8).

$$f(x, y) + b(x, y) = g(\tilde{x}, \tilde{y}), \quad (2.8)$$

where $b(x, y)$ is the value of the defect caused by the photograph. If such defects represented by the function $b(x, y)$ occur very rarely, we can approximate Eq. (2.8) with Eq. (2.9).

$$R(x, y) = \sum_{S_p \in S} \left[f(x, y) - g(\tilde{x}, \tilde{y})\right]^2, \quad (2.9)$$

where S represents the total number in the considered frame and S_p represents a single point of each point in the considered frame. Then, we will use the Least Square Method to compare between the deformed image and non-deformation image that can be written from Eq. (2.10)

$$\nabla R = \frac{\partial R}{\partial \boldsymbol{u}} = 0, \qquad (2.10)$$

where the vector $\boldsymbol{u}$ is $\left[u, \frac{\partial u}{\partial x}, \frac{\partial u}{\partial y}, v, \frac{\partial v}{\partial x}, \frac{\partial v}{\partial y}\right]^T$, ∇R is the gradient of R.

From Eq. (2.10), we find that when we substitute Eq. (2.10), it is a non-linear equation. Then, we can use the Newton-Raphson equation to solve Eq. (2.10) into a linear system as shown in Eq. (2.11).

$$\boldsymbol{u} = \boldsymbol{u}_0 - \left\{\left[\nabla\nabla R(\boldsymbol{u}_0)\right]^{-1}\left[\nabla R(\boldsymbol{u}_0)\right]\right\}, \quad (2.11)$$

where u_0 is the initial value of the problem and the vector u is the next value used to approximate the value in Eq. (2.10) and $\nabla\nabla R$ is the square value of the gradient. The second derivative is called the Hessian matrix, proposed by [3]. The Hessian matrix is used in a way that approaches zero; this will cause the matrix to not have divergence problems.

In addition, we will apply DIC for calculating material properties. We focus on the verification of the accuracy simulation results of the digital image reconstruction method. We use the existing program that was proposed by [1] by applying the MATLAB program to study the effect of changing the number and size in image pixels of speckle granules to compare the result of the material properties between using the

digital image correction method (DIC) and the standard average of material properties.

The problem analysis in this research for plates with a hole drilled in the center. From Fig. 3 is an isotropic image of an infinitely sized work plate with circular holes subjected to tensile force which was presented by Barber [4-7] who presented the relationship equation as Eq. (2.12)

$$u_r = \frac{Tr\cos 2\theta}{2E}\left[(1+\vartheta) + \frac{4a^2}{r^2} - (1+\vartheta)\frac{a^4}{r^4}\right] + \frac{Tr}{2E}\left[(1-\vartheta) + (1+\vartheta)\frac{a^2}{r^2}\right],$$

$$u_\theta = \frac{Tr\sin 2\theta}{2E}\left[(1+\vartheta) + 2(1-\vartheta)\frac{a^2}{r^2} + (1+\vartheta)\frac{a^4}{r^4}\right], \quad (2.12)$$

where T is the stress or surface traction, r is the distance measured from the center of the drill hole to the point where removal is to be measured, E is the material constant (Young's Modulus), ϑ is Poisson's Ratio and a is the hole radius of the workpiece. The polar coordinates can be changed to coordinates along the x and y axes using Eq. (2.13).

$$u(x,y) = u_r\cos\theta - u_\theta\sin\theta,$$
$$v(x,y) = u_r\sin\theta - u_\theta\cos\theta, \quad (2.13)$$

where $u(x,y)$ is the x-axis displacement and $v(x,y)$ is the y-axis displacement. We can change from polar coordinates to x and y axis coordinates.

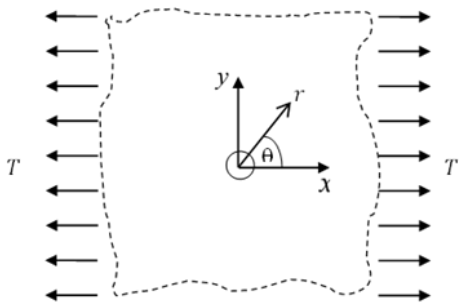

Fig. 3. An infinite plate with a hole drilled in the center [1].

Modeling of digital image reconstruction is a very popular method because the steps and methods are not difficult. For example, research by [8] mentioned that modeling only requires a computer that can test the accuracy of digital image reconstruction algorithms. However, the research tests did not account for errors caused by digital cameras and the entire system.

As for the equation used to simulate the image created by the removal on the material, we can do it using Eq. (2.14) as shown.

$$f(x,y) = \sum_{k=1}^{s} I_k^0 exp\left[-\left(\left(x-x_k\right)^2 + \left(y-y_k\right)^2\right)/R^2\right],$$
$$g(x',y') = \sum_{k=1}^{s} I_k^0 exp\left[-\left(\frac{\left(x-x_k-u_0-u_x x-u_y y\right)^2 + \left(y-y_k-v-v_x x-v_y y\right)^2}{R^2}\right)\right],$$

where $f(x,y)$ and $g(x',y')$ are the color intensity points of each pixel in the image of non-displacement and displacement respectively. s is the number of speckle granules. R is the size of the image spots. $\left(x_k, y_k\right)$ is the position of each point that is randomly distributed. I_k^0 is the random maximum color intensity of each image spot. $\left(u_0, v_0\right)$ is displacement in the x and y axes, respectively. u_x, v_y are the stress values in the x and y axes, respectively. u_y, v_x are the shear stress values in the x and y axes, respectively.

2.1 Speckle simulation

In the experiment, we will use Eq. (2.14) to simulate an image with the number of image pixels (s) equal to 5,000 and the color level of the image equal to 16 bits and each pixel size 0.06 mm. The simulation results will be as follows from Fig.4.

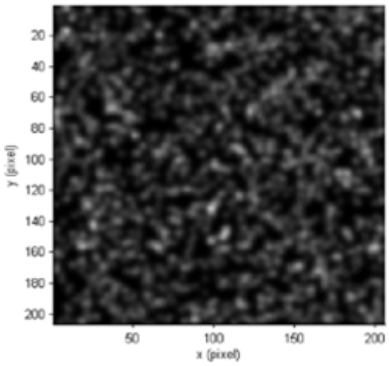

Fig. 4. The simulation of image points.

2.2 Q4-Digital Image Correlation method (Q4-DIC)

A technique introduced by [5] compares the surface picture of two images to be examined. In the first picture it is called surface picture before deformation and the second picture is called surface picture after deformation that both surface pictures are in the coordinate system in the form of a scalar function. It can be seen from the gray dot image in each pixel that $f(x)$ is the image before deformation and $g(x)$ is the image after deformation of the test specimen that can be written as a relationship Eq. (2.15).

$$g(x) = f\left[x + \boldsymbol{u}(\boldsymbol{x})\right], \qquad (2.15)$$

where $u(x)$ is a displacement of the test specimen, f and g are the displacement differences between the specimens. For a small displacement, we can use the first order Taylor's equation to find the components and find the point of error from Eq. (2.16).

$$R = g(x) - f(x) - u(x) \bullet \nabla f(x), \quad (2.16)$$

For functions that have a rhombus shape in each element We can use Eq. (2.17) to help find this. This equation was presented by [9].

$$u(x) = \Phi \mathrm{U}, \qquad (2.17)$$

where the matrix Φ is stored in the form of a shape function represented by $\left(\varnothing_1, \varnothing_2, \varnothing_3, \varnothing_4\right)$ and the matrix U is stored as 8 displacements $\left(U_1, V_1, \ldots, U_4, U_4\right)$.

Where the coordinates are in the form of square $[0,1]^2$ can be written as 4 functions: $(1-x)(1-y)$, $x(1-y)$, $y(1-x)$ and xy.

Next, we are interested in the zone of interest (ZOI), which is the zone that we are interested in considering conducting experiments by creating models for use in calculating the properties of materials in that zone. These are stored in domain form and can be written as $\Omega \subset \Re^2$. For small domain areas it is written as Ω^e where $\Omega^e \subset \Omega$. We need to use the least square method to combine the remaining components together, expressed in the form of Eq. (2.18).

$$\frac{\partial}{\partial \boldsymbol{U}} \int_{\Omega^e} \Re^2 d\Omega, \qquad (2.18)$$

From Figs. 5 A and B, we will show how to divide the zones that we are interested in considering into subsets. We use Eq. (2.18) that we obtained from the least squares method to apply it linearly. We will get Eq. (2.19).

$$\int_{\Omega^e} k^T k d\Omega \boldsymbol{U} = \int_{\Omega^e} k^T (g - f)\, d\Omega, \qquad (2.19)$$

where the vector k can be replaced by $\left[\varnothing_1 \frac{\partial f}{\partial x}, \varnothing_1 \frac{\partial f}{\partial y}, \ldots, \varnothing_4 \frac{\partial f}{\partial x}, \varnothing_4 \frac{\partial f}{\partial y}\right]$ and the reference gradients in the x and y directions are $\frac{\partial f}{\partial x}$ and $\frac{\partial f}{\partial y}$ which can be solved by integrate from each pixel form Eq. (2.20).

$$K^e U^e = F^e, \qquad (2.20)$$

where the matrix elements K^e and F^e are composed of the Global Stiffness Matrix K and the force of matrix F. Then, we use finite elements to solve this equation for a small subpixel.

In this research, we will use the Bicubic Spine method to increase the

accuracy in calculating the surface pixel before deformation and after deformation. This method is in the form of the function $\left[-\frac{1}{2},\frac{1}{2}\right]^2$ which can be written in the polynomial form which was introduced by [10] as in Eq. (2.21).

$$f(\tilde{x},\tilde{y}) = \sum_{i=0}^{3}\sum_{j=0}^{3} a_{ij}\tilde{x}^{i}\tilde{y}^{i},$$

$$g(\tilde{x},\tilde{y}) = \sum_{i=0}^{3}\sum_{j=0}^{3} b_{ij}\tilde{x}^{i}\tilde{y}^{j}, \qquad (2.21)$$

where a_{ij} and b_{ij} are spine coefficients. which can be calculated from the linear equation in Eq. (2.22).

$$A \bullet b = C, \qquad (2.22)$$

where b has a dimension 16×1, spine coefficients $\left[a_{00}, a_{10}, a_{20}, \ldots, a_{33}\right]^T$ and C has a dimension 16×1 that stored as gray pixels displayed in a gradient $\left(f, \frac{\partial f}{\partial \tilde{x}}, \frac{\partial f}{\partial \tilde{y}}, \frac{\partial^2 f}{\partial \tilde{x}\partial \tilde{y}}\right)$ with the following nodes $\left(-\frac{1}{2},-\frac{1}{2}\right),\left(\frac{1}{2},-\frac{1}{2}\right),\left(-\frac{1}{2},\frac{1}{2}\right)$ and $\left(\frac{1}{2},\frac{1}{2}\right)$. We can use finite elements to find $\left(f, \frac{\partial f}{\partial \tilde{x}}, \frac{\partial f}{\partial \tilde{y}}, \frac{\partial^2 f}{\partial \tilde{x}\partial \tilde{y}}\right)$ for each pixel. Therefore, matrix A has size 16×16, represented by the positions of the nodes $\tilde{x}$ and $\tilde{y}$ from Eq. (2.19).

The integration equation from Eq. (2.19) is not easily evaluated directly due to the large number of elements of the Ω^s as a spire function. where element location points can be replaced by spire function points which is at the center of the spire square form by the integral Eq. (2.22) of the left and right elements can be represented by Eq. (2.23), which was introduced by [11].

$$\int_{\Omega^e} k^T k d\Omega U = \sum_{i=1}^{n}\int_{\Omega_i^s} k^T k \, det J d\Omega,$$

$$\int_{\Omega^e} k^T(g-f)\,\Omega U = \sum_{i=1}^{n}\int_{\Omega_i^s} k^T(g-f)\,det J d\Omega, \qquad (2.23)$$

where i is number of spire functions from 1 to n, where J element is equal to a 2×2 matrix that is a Jacobian matrix.

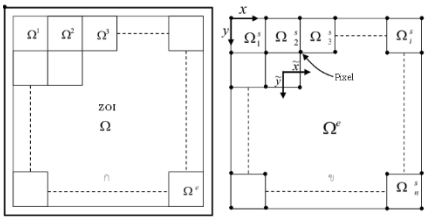

Fig. 5. (A) The zone of interest is composed of many elements in the domain. (B) The figure shows the subdomains that are subsets of the spire function.

2.3 Determine material properties using digital image correlation (DIC) with MATLAB.

We will use simulation testing by creating a simulation specimen by simulating the workpiece between undeformed and deformed workpiece to determine the material properties. This research uses computer simulation to determine material properties. The simulation was performed by specifying the test properties as shown in Fig. 6.

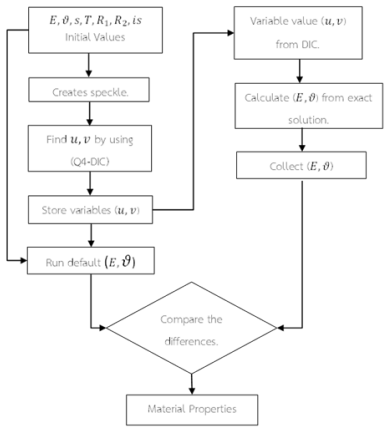

Fig. 6. Diagram showing the operation of the MATLAB program and the steps for finding material properties.

3. Results and Discussion

Results of testing for changing the number of speckle granules (s).

This test studied the effect of changing the number of speckle granules for determining material properties using the Digital Image Correction method and comparing the results with the standard average of material properties.

This test used stainless steel - grade 304 (UNS S30400) by testing 3 sets of experiments with an unequal number of speckle granules in each test to compare the result between Digital Image Correlation and the standard of material properties.

Table 1. The conditions of stainless steel - grade 304.

Name of variable	Value of variable
Poisson's Ratio: ϑ	0.275
Young's Modulus: E	203 GPa
Radius of central hole: a	2 mm
Stress or Surface Traction: T	8.8164 MPa
Total Speckle Granular: s	3000
Image size: pixel: is	206

From Table 1, when we calculated through the GUI in MATLAB by applying the digital image correction method to calculate, the test results for changing the number of speckle granules are obtained as shown in Tables 2-4.

Table 2. The table shows tests using the number of speckle granules equal to 3000 points.

Number	Young's Modulus	Poisson's Ratio
1	203.140	0.2770
2	203.260	0.2750
3	203.270	0.2450
4	203.270	0.2720
5	203.180	0.2730
6	203.050	0.2710
7	203.010	0.2740
8	203.050	0.2740
9	203.030	0.2760
10	203.040	0.2790
Average	203.130	0.2716

Table 3. The table shows tests using the number of speckle granules equal to 5000 points.

Number	Young's Modulus	Poisson's Ratio
1	203.340	0.2740
2	203.030	0.2760
3	203.110	0.2750
4	203.080	0.2770
5	203.010	0.2730
6	203.080	0.2750
7	203.070	0.2710
8	203.220	0.2780
9	203.130	0.2750
10	203.060	0.2740
Average	203.113	0.2748

Table 4. The table shows tests using the number of speckle granules equal to 7000 points.

Number	Young's Modulus	Poisson's Ratio
1	203.010	0.2751
2	203.010	0.2753
3	203.040	0.2749
4	203.020	0.2753
5	203.060	0.2750
6	203.040	0.2756
7	203.010	0.2748
8	203.020	0.2750
9	203.090	0.2750
10	203.050	0.2760
Average	203.035	0.2752

Tables 5-6 show the average of Young's Modulus and Poisson's Ratio from unequal number of speckle granules.

Table 5. Compare the varied number of speckle granules between standard material properties and Digital Image Correlation (DIC). (Young's Modulus)

Number of speckle granules; s	Young's Modulus (standard)	Young's Modulus (DIC)
3000	203	203.130
5000	203	203.113
7000	203	203.035

Table 6. Compare the varied number of speckle granules between standard material properties and Digital Image Correlation (DIC). (Poisson's Ratio)

Number of speckle granules; s	Poisson's Ratio (standard)	Poisson's Ratio (DIC)
3000	0.2750	0.2716
5000	0.2750	0.2748
7000	0.2750	0.2752

Tables 7-8 show the percent error of Young's Modulus and Poisson's Ratio from unequal number of speckle granules.

Table 7. Percent error of Young's Modulus between standard material properties and Digital Image Correlation.

Number of speckle granules; s	Young's Modulus (Standard)	Young's Modulus (DIC)	Percent error (%)
3000	203	203.130	0.063998425
5000	203	203.113	0.055634056
7000	203	203.035	0.017238407

Table 8. Percent error of Poisson's Ratio between standard material properties and Digital Image Correlation.

Nnumber of speckle granules; s	Poisson's Ratio (Standard)	Poisson's Ratio (DIC)	Percent error (%)
3000	0.2750	0.2716	1.251840943
5000	0.2750	0.2748	0.072780204
7000	0.2750	0.2752	0.072674419

Results of testing for changing the size of speckle granules (s) in the same condition from Table 1 and the test results for changing the size of speckle granules are obtained as shown in Tables 9-11.

Table 9. The table shows tests using the size of speckle granules equal to 1 mm.

Number	Young's Modulus	Poisson's Ratio
1	203.8900	0.27490
2	203.0100	0.27660
3	203.8600	0.27840
4	203.0100	0.27600
5	203.0200	0.27780
6	204.4400	0.27490
7	204.6200	0.27610
8	203.7800	0.27640
9	203.4800	0.27650
10	203.3300	0.27710
Average	203.6440	0.27647

Table 10. The table shows tests using the size of speckle granules equal to 3 mm.

Number	Young's Modulus	Poisson's Ratio
1	203.0420	0.2747
2	203.0110	0.2754
3	203.1240	0.2756
4	203.0130	0.2751
5	203.0020	0.2755
6	203.0220	0.2742
7	203.0860	0.2753
8	203.1640	0.2756
9	203.0820	0.2755
10	203.0780	0.2750
Average	203.0624	0.27519

Table 11. The table shows tests using the size of speckle granules equal to 5 mm.

Number	Young's Modulus	Poisson's Ratio
1	203.5450	0.2766
2	203.2130	0.2776
3	203.1260	0.2766
4	203.4130	0.2744
5	203.5060	0.2751
6	203.4260	0.2786
7	203.5890	0.2751
8	203.3360	0.2761
9	203.4540	0.2753
10	203.4450	0.2750
Average	203.4053	0.27604

Tables 12-13 show the average of Young's Modulus and Poisson's Ratio from unequal size of speckle granules.

Table 12. Compare the varied size of speckle granules between standard material properties and Digital Image Correlation (DIC). (Young's Modulus)

Size of speckle granules; R	Young's Modulus (standard)	Young's Modulus (DIC)
1	203	203.6440
3	203	203.0624
5	203	203.4053

Table 13. Compare the varied size of speckle granules between standard material properties and Digital Image Correlation (DIC). (Poisson's Ratio)

Size of speckle granules; R	Poisson's Ratio (standard)	Poisson's Ratio (DIC)
1	0.27500	0.27647
3	0.27500	0.27519
5	0.27500	0.27604

Tables 14-15 show the percent error of Young's Modulus and Poisson's Ratio from unequal size of speckle granules.

Table 14. Percent error of Young's Modulus between standard material properties and Digital Image Correlation (DIC).

Size of speckle granules; *R*	Young's Modulus (Standard)	Young's Modulus (DIC)	Percent error (%)
1	203	203.6440	0.316238141
3	203	203.0624	0.030729470
5	203	203.4053	0.199257345

Table 15. Percent error of Poisson's Ratio between standard material properties and Digital Image Correlation (DIC).

Size of speckle granules; *R*	Poisson's Ratio (Standard)	Poisson's Ratio (DIC)	Percent error (%)
1	0.27500	0.27647	0.531703259
3	0.27500	0.27519	0.069043207
5	0.27500	0.27604	0.376756992

4. Conclusion

In conclusion, Digital Image Correlation (DIC) continues to be a valuable tool for researchers and practitioners, offering unprecedented insights into the mechanics and behavior of materials and structures. In this research, if we have only images, the DIC can be used to predict the Young's Modulus and Poisson's Ratio. The results show that the errors of changing the number of speckle granules from Digital Image Correlation (DIC) in Young's Modulus (E) around 0.017238407-0.063998425% and Poisson's ratio (ϑ) around 0.072674419-1.251840943% and the errors of changing the size in image pixels of speckle granules from Digital Image Correlation (DIC) in Young's Modulus (E) around 0.030729470-0.316238141% and Poisson's ratio (ϑ) around 0.069043207-0.531703259%.

However, number of speckle granules, the optimum number of speckle granules to use should be in the range of 3000-5000 pixels to provide accurate feature values and significantly reduce processing time.

In addition, if we change the size of speckle granules to be equal to 5 mm, it will be found that the error of displacement is greater than the size of speckle granules equal to 3 mm but less than size 1 mm because the size of speckle granules equal to 5 mm has a size and movement that can be captured more easily than size 1 mm.

As a result, the calculation results compared with 3 mm found that the size of speckle granules should be between 2-4 mm to get good tolerances, resulting in more accurate material property predictions.

Acknowledgments

I would like to express my deepest gratitude to the following individuals and organizations who have contributed to the success of this research.

For Associate Professor Dr. Prapot Kunthong: I am immensely thankful for the guidance, support, and invaluable insights provided by my best advisor. Your mentorship has been instrumental in shaping the direction of this research.

For Dr. Rittipol Chantarat: I extend my appreciation to my peers who have shared their expertise, ideas, and constructive feedback throughout the course of this project. Your collaboration has enriched the quality of the research.

For Pathumwan Institute of Technology and Kasetsart University: This research was made possible through the financial support of Pathumwan Institute of Technology and Kasetsart University. Their investment in this project has been crucial for its successful completion.

For my family (Mrs. Wattana Kaoroptham and Mr. Sompoch Kaoroptham): To my family, your unwavering support, encouragement, and understanding have been my pillars of strength. Thank you for being there for me during the highs and lows of this research journey.

Finally, I am grateful to everyone who played a role in making this research a

reality. Your support has been instrumental, and I appreciate each one of you for your contributions.
Thank you.

References

[1] Rittipol, C. and Prapot, K. 2013. Mix Numerical-Experimental Technique for identification of constitutive parameters. pp.11- 25.

[2] Lecompte D, A. Smits, S. Bossuyt, H. Sol, J. Vantomme, D. Van Hemelrijck and A.M. Habraken. Quality assessment of speckle patterns for digital image correlation. Optics and Lasers in Engineering 2006;44(11):1132-45.

[3] Hung, P.-C. and A.S. Voloshin. In-Plane Strain Measurement by Digital Image Correlation. J. of the Braz. Soc. of Mech. Sci. & Eng. 2003;25(3):215-21.

[4] Barber, J.R. 2002. Elasticity. 2nd Edition. Kluwer Academic Publishers, Netherlands.

[5] Besnard G, F. Hild and S. Roux. "Finite-Element" displacement fields analysis from digital images: application to Portevin–Le Châtelier bands. Experimental Mechanics 2006;46(6):789-803.

[6] Bornert M, F. Brémand, P. Doumalin, J.C. Dupré, M. Fazzini, M. Grédiac, F. Hild, S. Mistou, J. Molimard, J.J. Orteu, L. Robert, Y. Surrel, P. Vacher and B. Wattrisse. Assessment of digital image correlation measurement errors: methodology and results. Experimental Mechanics 2009;49(3):353-70.

[7] Timoshenko S. and J.N. Goodier. 1969. Theory of Elasticity. McGraw-Hill.

[8] Bing P, X. Hui-min, X. Bo-qin and D. Fu-long. Performance of sub-pixel registration algorithms in digital image correlation. Meas. Sci. Technol. 2006;17(6):1615-21.

[9] Reddy J. 2005. An Introduction to the Finite Element Method. McGraw-Hill.

[10] Lancaster P. and K. Šalkauskas. 1986. Curve and Surface Fitting: An Introduction. Academic Press, Great Britain.

[11] Zill, D. and W. Wright. 2011. Multivariable Calculus. Jones & Bartlett Learning.